Paleoceanography & Paleoclimatology

Supporting Information for

The temperature of the deep ocean is a robust proxy for global mean surface temperature during the Cenozoic

David Evans[1], Julia Brugger[2], Gordon N. Inglis[1], Paul Valdes[3]

[1]School of Ocean and Earth Science, University of Southampton, Southampton, SO14 3ZH, UK
[2]Senckenberg Biodiversity and Climate Research Centre (SBiK-F), 60325 Frankfurt am Main, Germany
[3]School of Geographical Sciences, University of Bristol, Bristol, BS8 1SS, UK

Contents of this file

Introduction

This supplementary file contains information on the derivation of main text Fig. 2 (Text S1), an overview of the key nonthermal influences on the three principal deep ocean temperature proxies (Text S2), and details of the calculation of the theoretical relationship between foraminifera $\delta^{18}O$ and seawater pH (Text S3).

Text S1. Calculation of the idealized relationship between high latitude SST and global mean surface temperature (main text Fig. 2).

Surface area-weighted temperature for a zonally homogeneous sphere was calculated by: i) defining a temperature difference between the equator and pole, between which temperature varies linearly and continuously as a function of latitude, ii) calculating surface-area weightings according to the relationship between surface area and latitude on a sphere, and iii) multiplying the two together to derive global average and high latitude surface temperature, the latter defined as being 65 to 80°.

The aim of the exercise is to determine what relationship between global average and high latitude temperature is expected for differential degrees of tropical versus high latitude warming. To do so, we first calculate the surface area-weighted temperatures for a 'control' planet, with a surface temperature of -10°C and 25°C at the poles and equator respectively. Then, the temperature of the equator, pole, or both is raised incrementally to define a new latitude-temperature relationship and surface area-weighted temperature is recomputed. Finally, the ratio of the change in surface area-weighted GMST to the change in surface area-weighted high latitude temperature is calculated, which is the ratio of GMST change relative to the control planet to the high latitude temperature change relative to high latitude in the control planet. Doing so over a wide range of changes in tropical and high latitude temperature results in the contours shown in main text Fig. 2A. Main text Fig. 2B presents an identical calculation except with an artificial temperature bias added to the surface area-weighted high latitude temperature of -1°C per 5°C GMST increase, here intended to represent a bias of deep ocean temperature away from high latitude SST due to a seasonal bias in deep water formation. This relationship (-1/5°C) was chosen to illustrate the approximate magnitude of the bias necessary to explain some Eocene data (see Fig. 2B) in the absence of any other process, and does not necessarily have a real-world basis. The code used to generate Fig. 2 (and all other main text figures) can be found at https://zenodo.org/record/xxxxxxx.

Text S2. Known strengths, weaknesses, and nonthermal controls on the three key benthic foraminifera-derived bottom water temperature proxies.

The oxygen isotopic composition of benthic foraminifera (abbreviated $\delta^{18}O$) forms the backbone of a large portion of palaeoceanography (e.g. Billups and Schrag, 2003; Emiliani, 1966; Shackleton, 1967; Westerhold et al., 2020; Zachos et al., 2001). The methodology is rooted in the temperature-dependent fractionation of ^{18}O relative to ^{16}O between water and the dissolved inorganic carbon species that react to form $CaCO_3$, with a slope of ~0.25‰/°C. As applied to deep benthic foraminifera, the proxy is very weakly sensitive to diagenesis in most settings because i) recrystallisation of the shell, if an issue, generally takes place in the early stages of burial during which the temperature of the pore water (and the overlying ocean) is similar to that when the foraminifera lived, and ii) because most benthic foraminifera precipitate $CaCO_3$ reasonably close in isotopic composition to diagenetic calcite (Evans et al., 2018; Raymo et al., 2018). The major limitation of the proxy when interpretation purely in terms of temperature is desirable is

that the oxygen isotopic composition of seawater varies both temporally, as the amount of water stored on land changes through time, and spatially, driven by the balance between precipitation (isotopically heavy) and evaporation (isotopically light). This latter issue is naturally a far greater issue for surface environments, with the variability of deep ocean $\delta^{18}O_{sw}$ equal to 0.48‰, equivalent to ~±2°C (2SD of all measurements >3000 m depth available at https://data.giss.nasa.gov/o18data/ excluding the Mediterranean (Bigg and Rohling, 2000; Schmidt, 1999)). However, changes in continental ice and groundwater storage through time can be challenging to deconvolve from temperature (see e.g. Eqs 1.1-1.3) and have driven changes in bulk seawater of at least a permil (~4°C). In addition, a seawater carbonate chemistry effect on foraminiferal $\delta^{18}O$ has been described in the case of planktonic foraminifera (Spero et al., 1997). This effect is rooted in the pH-dependent proportion of HCO_3^- versus CO_3^{2-} in seawater, important because the two species are characterised by distinct isotopic fractionations relative to H_2O (Zeebe, 1999) and implying that the phenomenon should be ascribed to pH rather than $[CO_3^{2-}]$. While the presence of a pH control on benthic foraminiferal $\delta^{18}O$ is yet to be conclusively demonstrated, our firm understanding of the mechanistic basis of this effect (Zeebe, 1999) means that it is likely to impact the oxygen isotopic composition of organisms other than planktonic foraminifera, such that the impact of pH on the benthic foraminifera $\delta^{18}O$ stack should at least be considered (Meckler et al., 2022).

The magnesium to calcium ratio of benthic foraminifera is sensitive to temperature likely in part because Mg substitution for Ca is increasingly thermodynamically favoured at higher temperature (Lea et al., 1999) and as a result of poorly understood biological processes. Foraminiferal Mg/Ca is not sensitive to orbital-scale changes in seawater chemistry but is complicated by a number of factors including: i) the long term variability of seawater Mg/Ca (Mg/Ca_{sw}) on multi-Myr timescale (Evans and Müller, 2012; Lear et al., 2000), which must be accounted for, ii) preferential diagenetic loss of Mg (Martin et al., 2002) or Mg increase via authigenic overgrowths (Pena et al., 2005), and iii) a possible additional seawater carbonate chemistry effect on Mg incorporation in some species (e.g. Elderfield et al., 2006). In addition, it is unfortunate that the regression form and/or slope of the relationship between Mg/Ca and temperature remains poorly constrained for some species that are widely used in paleoceanography (Cramer et al., 2011; Evans and Müller, 2012; Lear et al., 2015; Mawbey et al., 2020). Nonetheless, Mg/Ca data have been successfully coupled with $\delta^{18}O$ to deconvolve the relative contributions of $\delta^{18}O_{sw}$ and temperature on the latter proxy (Elderfield et al., 2012; Sosdian and Rosenthal, 2009), particularly when site-specific calibrations are employed (Woodard et al., 2014).

The clumped isotopic composition (Δ_{47}) of benthic foraminifera is based on the temperature-dependent degree to which two heavy isotopes bond ('clump') to each other, in this case ^{13}C and ^{18}O in CO_3 (Affek, 2012; Ghosh et al., 2006). Because it is the degree of clumping relative to the theoretical stochastic distribution of these isotopes that is measured, knowledge of $\delta^{18}O_{sw}$ is not required and the proxy does not suffer from uncertainty derived from potential changes in solution isotopic composition, in contrast to $\delta^{18}O$. For the same reason described above in relation to $\delta^{18}O$, Δ_{47} applied to benthic foraminifera is also insensitive to diagenesis (Leutert et al., 2019). The principal

disadvantage of the technique is that $^{13}C^{18}O^{16}O_2$ is a rare molecule (44 ppm of evolved CO_2), which means that the reproducibility of the measurements is driven by analytical repeatability to a far greater degree than other temperature proxies (Evans, 2021). In practical terms, the achievable precision of Δ_{47}-derived temperatures from benthic foraminifera is ~3-4°C (Meckler et al., 2022), such that resolving temperature changes of a magnitude lower than this may be challenging, or requires very large samples.

Text S3. Deriving a theoretical slope between pH and $\delta^{18}O$ (main text Sec. 4).

Following Zeebe et al. (1999), we calculate an approximate linear relationship between pH and $\delta^{18}O$ using the following equations:

$$S = [H_2CO_3] + [HCO_3^-] + [CO_3^{2-}]$$

Where the concentration of these three dissolved carbonate species was calculated across a pH range of 6.3-8.7 (total scale), between which the relationship between the oxygen isotope fractionation between H_2O and the sum of the dissolved carbon species is approximately linear, by holding alkalinity constant (2000 µmol/kg) and varying DIC (1250-2500 µmol/kg) at S = 35, T = 10°C and a depth of 4000 m. Then, the relationship between the oxygen isotope fractionation factor between water and the sum of the three dissolved carbon species above:

$$\alpha_{(S\text{-}H2O)} = \exp(-6.10\times10^{-4} \ln(S/[CO_2]) + 0.03452) \quad \text{(Eq. 2 in Zeebe, 1999)}$$

Finally, the slope used here (-1.54 ‰ per pH unit) is the least-squares linear fit through the resulting data regressed against pH. The calculation is insensitive to temperature, with a 10°C increase driving a decrease in the slope of ~0.004.

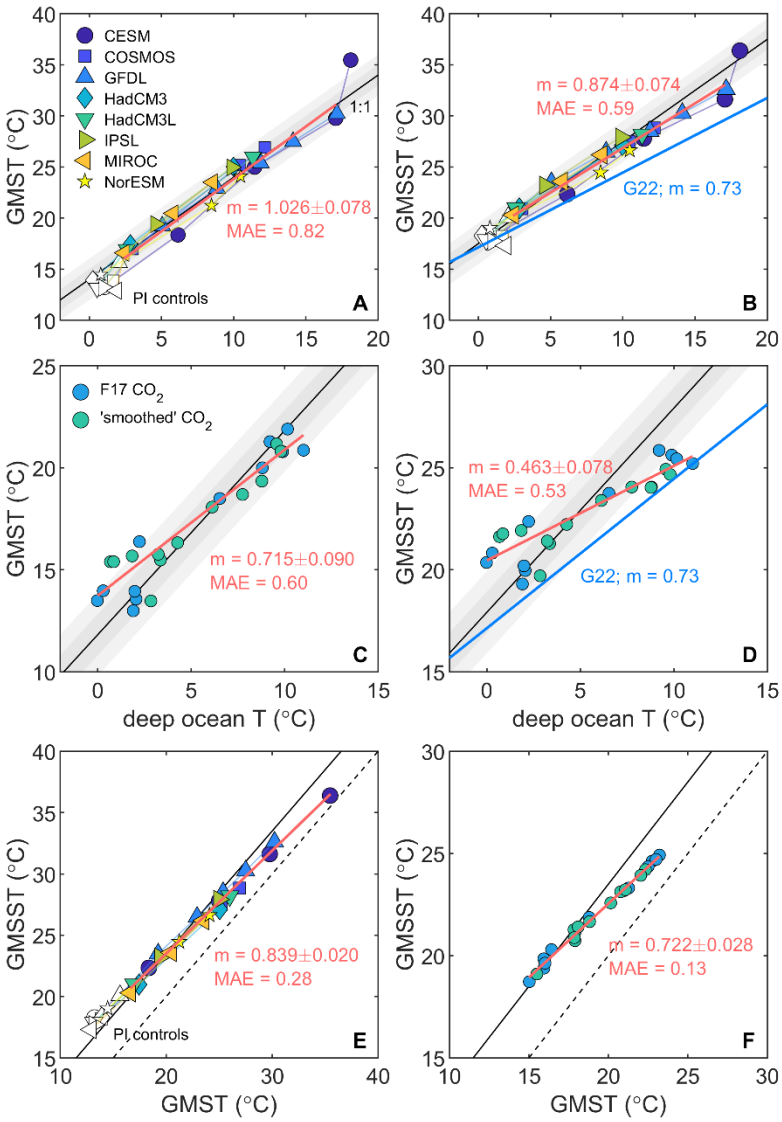

Figure S1. The same analysis as main text Fig. 4, with the exclusion of Arctic SST.

Table S1. The regions in which deep water formation takes place in the model simulations considered here. See main text Fig. 5 for the definition of these locations. These regions were used for simulations at all CO_2 and non-modern paleogeography. The mean annual and winter SST calculations in the main text use the same high latitude boxes.

	High latitude boxes in which deep water formation takes place				
	N. Atlantic	N. Pacific	S. Atlantic	S. Pacific	Indian sec.
CESM			■		■
COSMOS				■	
GFDL		■			
HadCM3			■		■
HadCM3L			■		■
IPSL			■	■	■
MIROC			■	■	■
NorESM			■		■
HadCM3$_{V21}$			■	■	■

References

Affek, H.P., 2012. Clumped Isotope Paleothermometry: Principles, Applications, and Challenges. The Paleontological Society Papers 18, 101–114. https://doi.org/10.1017/S1089332600002576

Bigg, G.R., Rohling, E.J., 2000. An oxygen isotope data set for marine waters. Journal of Geophysical Research: Oceans 105, 8527–8535. https://doi.org/10.1029/2000JC900005

Billups, K., Schrag, D.P., 2003. Application of benthic foraminiferal Mg/Ca ratios to questions of Cenozoic climate change. Earth and Planetary Science Letters 209, 181–195. https://doi.org/10.1016/S0012-821X(03)00067-0

Cramer, B.S., Miller, K.G., Barrett, P.J., Wright, J.D., 2011. Late Cretaceous–Neogene trends in deep ocean temperature and continental ice volume: Reconciling records of benthic foraminiferal geochemistry (δ18O and Mg/Ca) with sea level history. Journal of Geophysical Research: Oceans 116. https://doi.org/10.1029/2011JC007255

Elderfield, H., Ferretti, P., Greaves, M., Crowhurst, S., McCave, I.N., Hodell, D., Piotrowski, A.M., 2012. Evolution of Ocean Temperature and Ice Volume Through the Mid-Pleistocene Climate Transition. Science 337, 704–709. https://doi.org/10.1126/science.1221294

Elderfield, H., Yu, J., Anand, P., Kiefer, T., Nyland, B., 2006. Calibrations for benthic foraminiferal Mg/Ca paleothermometry and the carbonate ion hypothesis. Earth and Planetary Science Letters 250, 633–649. https://doi.org/10.1016/j.epsl.2006.07.041

Emiliani, C., 1966. Isotopic Paleotemperatures. Science 154, 851–857. https://doi.org/10.1126/science.154.3751.851

Evans, D., 2021. Deep Heat: Proxies, Miocene Ice, and an End in Sight for Paleoclimate Paradoxes? Paleoceanography and Paleoclimatology 36, e2020PA004174. https://doi.org/10.1029/2020PA004174

Evans, D., Badger, M.P.S., Foster, G.L., Henehan, M.J., Lear, C.H., Zachos, J.C., 2018. No substantial long-term bias in the Cenozoic benthic foraminifera oxygen-isotope record. Nat Commun 9, 2875. https://doi.org/10.1038/s41467-018-05303-4

Evans, D., Müller, W., 2012. Deep time foraminifera Mg/Ca paleothermometry: Nonlinear correction for secular change in seawater Mg/Ca. Paleoceanography 27. https://doi.org/10.1029/2012PA002315

Ghosh, P., Adkins, J., Affek, H., Balta, B., Guo, W., Schauble, E.A., Schrag, D., Eiler, J.M., 2006. 13C–18O bonds in carbonate minerals: A new kind of paleothermometer. Geochimica et Cosmochimica Acta 70, 1439–1456. https://doi.org/10.1016/j.gca.2005.11.014

Lea, D.W., Mashiotta, T.A., Spero, H.J., 1999. Controls on magnesium and strontium uptake in planktonic foraminifera determined by live culturing. Geochimica et Cosmochimica Acta 63, 2369–2379. https://doi.org/10.1016/S0016-7037(99)00197-0

Lear, C.H., Coxall, H.K., Foster, G.L., Lunt, D.J., Mawbey, E.M., Rosenthal, Y., Sosdian, S.M., Thomas, E., Wilson, P.A., 2015. Neogene ice volume and ocean temperatures: Insights from infaunal foraminiferal Mg/Ca paleothermometry. Paleoceanography 30, 1437–1454. https://doi.org/10.1002/2015PA002833

Lear, C.H., Elderfield, H., Wilson, P.A., 2000. Cenozoic Deep-Sea Temperatures and Global Ice Volumes from Mg/Ca in Benthic Foraminiferal Calcite. Science 287, 269–272. https://doi.org/10.1126/science.287.5451.269

Leutert, T.J., Sexton, P.F., Tripati, A., Piasecki, A., Ho, S.L., Meckler, A.N., 2019. Sensitivity of clumped isotope temperatures in fossil benthic and planktic foraminifera to diagenetic alteration. Geochimica et Cosmochimica Acta 257, 354–372. https://doi.org/10.1016/j.gca.2019.05.005

Martin, P.A., Lea, D.W., Rosenthal, Y., Shackleton, N.J., Sarnthein, M., Papenfuss, T., 2002. Quaternary deep sea temperature histories derived from benthic foraminiferal Mg/Ca. Earth and Planetary Science Letters 198, 193–209. https://doi.org/10.1016/S0012-821X(02)00472-7

Mawbey, E.M., Hendry, K.R., Greaves, M.J., Hillenbrand, C.-D., Kuhn, G., Spencer-Jones, C.L., McClymont, E.L., Vadman, K.J., Shevenell, A.E., Jernas, P.E., Smith, J.A., 2020. Mg/Ca-Temperature Calibration of Polar Benthic foraminifera species for reconstruction of bottom water temperatures on the Antarctic shelf. Geochimica et Cosmochimica Acta 283, 54–66. https://doi.org/10.1016/j.gca.2020.05.027

Meckler, A.N., Sexton, P.F., Piasecki, A.M., Leutert, T.J., Marquardt, J., Ziegler, M., Agterhuis, T., Lourens, L.J., Rae, J.W.B., Barnet, J., Tripati, A., Bernasconi, S.M., 2022. Cenozoic evolution of deep ocean temperature from clumped isotope thermometry. Science 377, 86–90. https://doi.org/10.1126/science.abk0604

Pena, L.D., Calvo, E., Cacho, I., Eggins, S., Pelejero, C., 2005. Identification and removal of Mn-Mg-rich contaminant phases on foraminiferal tests: Implications for Mg/Ca past temperature reconstructions. Geochemistry, Geophysics, Geosystems 6, Q09P02. https://doi.org/10.1029/2005GC000930

Raymo, M.E., Kozdon, R., Evans, D., Lisiecki, L., Ford, H.L., 2018. The accuracy of mid-Pliocene δ18O-based ice volume and sea level reconstructions. Earth-Science Reviews 177, 291–302. https://doi.org/10.1016/j.earscirev.2017.11.022

Schmidt, G.A., 1999. Forward modeling of carbonate proxy data from planktonic foraminifera using oxygen isotope tracers in a global ocean model. Paleoceanography 14, 482–497. https://doi.org/10.1029/1999PA900025

Shackleton, N., 1967. Oxygen Isotope Analyses and Pleistocene Temperatures Re-assessed. Nature 215, 15–17. https://doi.org/10.1038/215015a0

Sosdian, S., Rosenthal, Y., 2009. Deep-Sea Temperature and Ice Volume Changes Across the Pliocene-Pleistocene Climate Transitions. Science 325, 306–310. https://doi.org/10.1126/science.1169938

Spero, H.J., Bijma, J., Lea, D.W., Bemis, B.E., 1997. Effect of seawater carbonate concentration on foraminiferal carbon and oxygen isotopes. Nature 390, 497–500. https://doi.org/10.1038/37333

Westerhold, T., Marwan, N., Drury, A.J., Liebrand, D., Agnini, C., Anagnostou, E., Barnet, J.S.K., Bohaty, S.M., Vleeschouwer, D.D., Florindo, F., Frederichs, T., Hodell, D.A.,

Holbourn, A.E., Kroon, D., Lauretano, V., Littler, K., Lourens, L.J., Lyle, M., Pälike, H., Röhl, U., Tian, J., Wilkens, R.H., Wilson, P.A., Zachos, J.C., 2020. An astronomically dated record of Earth's climate and its predictability over the last 66 million years. Science.

Woodard, S.C., Rosenthal, Y., Miller, K.G., Wright, J.D., Chiu, B.K., Lawrence, K.T., 2014. Antarctic role in Northern Hemisphere glaciation. Science 346, 847–851. https://doi.org/10.1126/science.1255586

Zachos, J., Pagani, M., Sloan, L., Thomas, E., Billups, K., 2001. Trends, Rhythms, and Aberrations in Global Climate 65 Ma to Present. Science 292, 686–693. https://doi.org/10.1126/science.1059412

Zeebe, R.E., 1999. An explanation of the effect of seawater carbonate concentration on foraminiferal oxygen isotopes. Geochimica et Cosmochimica Acta 63, 2001–2007. https://doi.org/10.1016/S0016-7037(99)00091-5